

# Comparison of the thermal stability of magnesium phosphate (newberyite) coating with conventional zinc phosphate (hopeite) coating

## Porovnání tepelné stability hořečnatého fosfátu (newberyite) s konvenčním povlakem zinečnatého fosfátu (hopeite)

Pokorný P.

Czech Technical University – Klokner Institute

E-mail: Petr.Pokorny@cvut.cz

*This article presents a detail comparison of the thermal stability of the new magnesium phosphate (newberyite –  $MgHPO_4 \cdot 3H_2O$ ) coating with a conventional coating of zinc phosphate (hopeite –  $Zn_3(PO_4)_2 \cdot 4H_2O$ ). It was confirmed that dehydration of zinc phosphate (hopeite) occurs gradually (dehydration start temperature: 115 °C). The start of magnesium phosphate (newberyite) dehydration is indeed shifted to somewhat higher temperatures (about 125 °C) but the dehydration has an intense jump character. When using magnesium phosphate (newberyite) coating for further surface treatment at higher temperatures, dehydration of the coating can result in reduction of the adhesion between the phosphate/primer coatings. Under these conditions, it is recommended to use a coating of conventional zinc phosphate (hopeite) or manganese phosphate (hurealite).*

*Tento článek detailně porovnává tepelnou stabilitu krystalů nového povlaku hořečnatého fosfátu (newberyite –  $MgHPO_4 \cdot 3H_2O$ ) s běžně v praxi používaným povlakem zinečnatého fosfátu (hopeite –  $Zn_3(PO_4)_2 \cdot 4H_2O$ ). Bylo potvrzeno, že dehydratace zinečnatého fosfátu (hopeite) má postupnější charakter (vlastní dehydratační proces začíná při teplotě 115 °C). Počátek dehydratace hořečnatého fosfátu (newberyite) je posunut k mírně vyšším teplotám (přibližně 125 °C), ovšem dehydratace má významný skokový charakter. Použití následně povrchové úpravy aplikované za vyšších teplot na povlak hořečnatého fosfátu, může, vlivem intenzivní dehydratace krystalů fosfátu, snížit přilnavost finální povrchové úpravy. Pro praktické použití je z tohoto pohledu vhodnější použití konvenčního povlaku zinečnatého fosfátu (hopeite) nebo manganatého fosfátu (hurealite).*

### INTRODUCTION

Phosphate metal finishing is still considered the highest standard for the pretreatment of steel profiles before applying organic coatings [1]. These coatings form a suitable anchor profile for different systems of organic coatings and prolong the overall life of corrosion protection. This is achieved primarily because the treatment provides long-term protection from corrosion to the organic coating [2-6].

Phosphate coatings are usually crystalline and are clearly divided by the content characteristic of metal cation per molecule: zinc phosphating, zinc/calcium phosphating, manganese phosphating and iron phosphating (amorphous coating, only indicates crystal structure, the dominant phase is formed by  $Fe_3(PO_4)_2 \cdot 8H_2O$  – vivianite). The individual coatings differ from each other not only in crystal structure, but also specific coating weight ( $g/m^2$ ), grain morphology, toughness, cleavage, porosity, thermal stability and, finally, color [1, 2, 7, 8].

Heat stability, i.e. resistance of the crystalline coating to dehydration, is, in many respects, a key property of the phosphate coating. It is important first of all to verify the value of the initial dehydration and quantitative assessment of the degree of dehydration (the amount of evaporated molecules of  $H_2O$ ). Dehydration of the phosphate coating during deposition of the primer coating may negatively affect its bond (thermo-setting paint, plasma deposited coatings) [9].

Recent research confirms the possibility of using a new type of magnesium phosphate crystal based on bobierrite ( $Mg_3(PO_4)_2 \cdot 4H_2O$ ) and especially newberyite ( $MgHPO_4 \cdot 3H_2O$ ) for the corrosion protection of steel [10-12]. Furthermore, it has been verified that the  $MgHPO_4 \cdot 3H_2O$  coating can successfully precipitate on magnesium alloys [13-15]. Since it has been demonstrated that newberyite coatings provide comparable corrosion resistance to coatings based on conventional zinc phosphating (hopeite), it can therefore be a suitable alternative [11, 12].

In the context of comparing the properties of both types of coatings, it is necessary to compare their thermal stability. This study compared the thermal stability of both coatings via the DTA and TG methods.

## EXPERIMENTAL

Sheets of non-alloy steel ( $100 \times 100 \times 1 \text{ mm}^3$ ) were used as the basis for coating. Steel was first blasted with alumina abrasive (F240). Subsequently, the samples were degreased in a solution of 15 wt. % NaOH at  $70 \text{ }^\circ\text{C}$  for 5 minutes. This was followed by rinsing with deionized water, and pickling in 15 wt. % hydrochloric acid at  $50 \text{ }^\circ\text{C}$  for 2 minutes. Finally, the plates were rinsed in deionized water and phosphated in either a bath of conventional zinc phosphate or a bath of magnesium phosphate. The composition of the individual baths and the coating conditions are summarized in Tab. 1.

After drying, a total of 20 samples of each type were subjected to gravimetric analysis to determine the specific coating weight ( $\text{g}/\text{m}^2$ ) of the coatings. KERN ABJ analytical scales were used in the analysis and determination of the dimensions was made using a digital meter (KINEX Labo Iconic IP 67).

Before the thermal analysis, the morphology of the coatings was monitored using SEM and the identity and purity coating was confirmed by XRD. SEM scanning was carried out on the TESCAN Vega – 3LMU device. X-ray diffraction analysis was performed on a Bruker AXS D8 (scanning by Cu lamp).

After drying, the individual crystalline coatings were scraped from the surface of the coated steel with a fine ceramic brush. The scraping off of the crystalline coating was carried out very slowly in order to avoid friction heating of the steel substrate and any thermal

effect on the collected crystals. Prior to analysis, the samples were placed in a desiccator for 10 days for absolute drying. Measurement of thermal properties of individual phosphates was carried out on the Setari Set-Sys 1750 device. The temperature measurement range was set to approximately  $20\text{--}700 \text{ }^\circ\text{C}$  with a heating rate of about  $10 \text{ }^\circ\text{C}/\text{min}$ . Both samples were exposed in an environment with a nitrogen gas inlet of  $20 \text{ ml}/\text{min}$ . The weight of samples for TG/DTA analysis was comparable for both samples, i.e.,  $23.93 \text{ mg}$  in the case of the sample of magnesium phosphate and  $24.62 \text{ mg}$  in the case of zinc phosphate.

## RESULTS AND DISCUSSION

Table 2. summarizes the results of gravimetric analysis for both the phosphate coatings. From the results, it is evident that the two coatings provide very similar basis weight; however, the coating of magnesium phosphate (newberyite) statistically has a slightly lower weight. These results correlate well with the degree of surface coverage, even though zinc phosphate (hopeite) is slightly higher. Weight and degree of surface coverage is related to the smaller grain size of the zinc phosphate precipitate (see Figure 1 and Figure 2).

Tab. 2. Determination of the average specific coating weight ( $\text{g}/\text{m}^2$ ) of the phosphate coatings / Stanovení průměrné plošné hmotnosti ( $\text{g}/\text{m}^2$ ) obou druhů fosfátových povlaků

Sample type	Mg – phosphate (newberyite)	Zn – phosphate (hopeite)
average	3.21	3.69
standard deviation	0.18	0.24

Tab. 1. Chemical composition and operating conditions for zinc and magnesium phosphate baths (reprinted from [11]) / Chemické složení a pracovní podmínky lázně zinečnatého a hořečnatého fosfátu (převzato z [11])

Zinc phosphate bath	Magnesium phosphate bath
Bath composition	
$\text{H}_3\text{PO}_4$ (85 wt. %): 17 ml/l	$\text{H}_3\text{PO}_4$ (85 wt. %): 23 ml/l
ZnO: 2 g/l	$\text{MgCO}_3$ : 8.5 g/l
NaOH: 7g/l	$\text{NaNO}_2$ : 0.4 g/l
	NaOH: 7g/l
Operating conditions	
Temperature = $65 \text{ }^\circ\text{C}$	Temperature = $80 \text{ }^\circ\text{C}$
pH = 2.8	pH = 4.3
Time = 20 min	Time = 20 min

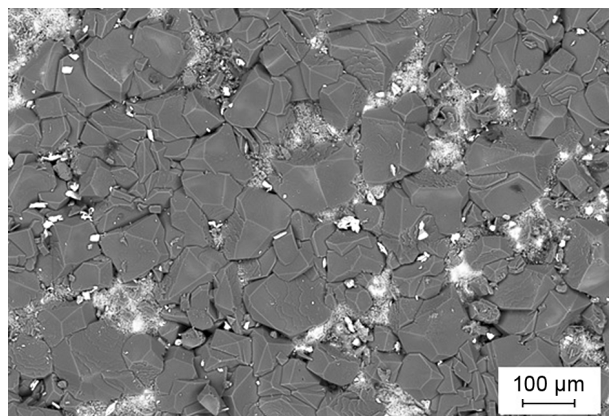


Fig. 1. SEM images of Mg – phosphate (newberyite) layer precipitated on conventional unalloyed steel – BSE visualization

Obr. 1. Snímek ze SEM povlaku Mg – fosfátu (newberyite) precipitovaného na povrchu uhlíkové oceli (BSE)

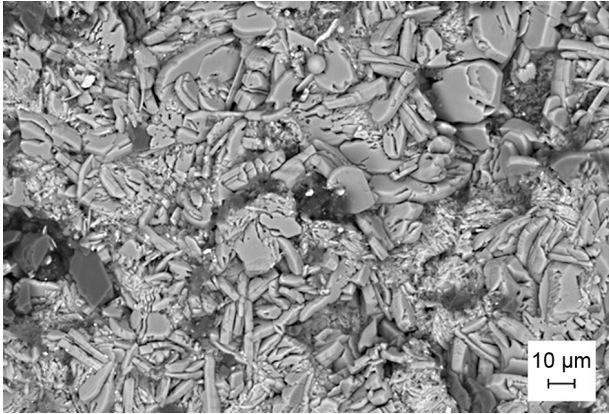


Fig. 2. SEM images of Zn – phosphate (hopeite) layer precipitated on conventional unalloyed steel – BSE visualization  
Obr. 2. Snímek ze SEM povlaku Zn – fosfátu (hopeite) precipitovaného na povrchu uhlíkové oceli (BSE)

Records from XRD confirmed the presence of pure forms of newberyite ( $\text{MgHPO}_4 \cdot 3\text{H}_2\text{O}$ ) formed on the surface of the alloy steel (see Figure 3) according to the following reaction [11, 12]:

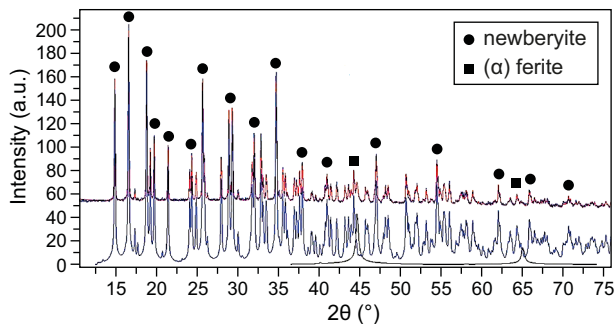
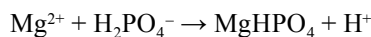


Fig. 3. X-ray diffraction patterns of Mg – phosphate (newberyite) layer on conventional unalloyed steel ((α) ferite)  
Obr. 3. Výsledky XRD fázové analýzy složení Mg-fosfátu (newberyite) precipitovaného na povrchu uhlíkové oceli ((α) ferite)

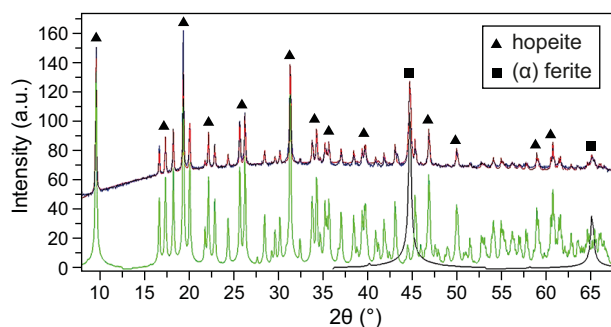
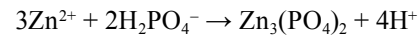


Fig. 4. X-ray diffraction patterns of Zn – phosphate (hopeite) layer on conventional unalloyed steel ((α) ferite)  
Obr. 4. Výsledky XRD fázové analýzy složení Zn-fosfátu (hopeite) precipitovaného na povrchu uhlíkové oceli ((α) ferite)

XRD confirmed the presence of only hopeite ( $\text{Zn}_3(\text{PO}_4)_2 \cdot 4\text{H}_2\text{O}$  – more precisely:  $\alpha$  modification) and not phosphophyllite ( $\text{Zn}_2\text{Fe}(\text{PO}_4)_2 \cdot 4\text{H}_2\text{O}$ ), although its presence cannot be excluded (see Figure 4.). The mixed phosphate is deposited as a minor phase (compared to hopeite) only in the layer near the steel substrate. Hopeite is formed according to the following reaction [2, 5]:



When comparing the specific coating weight ( $\text{g}/\text{m}^2$ ), degree of coverage and crystal size of both phosphate coatings, both can be attributed comparable anti-corrosion properties, which has been shown in [11].

The results of the comparative DTA analysis of both phosphate coatings are shown in Figure 5. The TG curve of the two coatings is shown in Figure 6. The initial decline of the DTA curve in “area 1” in the case of magnesium phosphate (newberyite) can be explained by a gradual dehydration of chemically unbound water (moisture) in the coating, and presumably the higher hygroscopic properties of newberyite crystals compared to hopeite crystals.

In “area 2” there is an obvious decrease in both curves indicating the progress of exothermic dehydration reactions. Although the dehydration reaction of the coating of magnesium phosphate (newberyite) runs at a slightly higher temperature (about  $125^\circ\text{C}$ ) than in the case of zinc phosphate (hopeite, about  $115^\circ\text{C}$ ), a considerably more vigorous dehydration is seen with magnesium phosphate coating.

At the larger multi-stage dehydration, the magnesium phosphate coating shows a strong decline in the curve in “area 3”. In this area, the decrease in the curve is slower, characterizing the thermal stability of zinc phosphate (hopeite). It can be assumed that dehydration when the temperature has not exceeded  $115^\circ\text{C}$  will be only partial and will continue until higher temperatures are reached. The initial temperature of dehydration of the zinc phosphate (hopeite) coating was set at an identical value as in other research [20, 22]. The curves of both phosphate coatings after the temperature exceeds  $250^\circ\text{C}$  are very similar (“area 4”), without any indication of exothermic dehydration reaction.

When comparing the TG-curves (Fig. 6) both phosphate coatings clearly confirm the fundamental conclusions above. If the temperature exceeds  $125^\circ\text{C}$  the weight pattern of the magnesium phosphate crystals decreases rapidly (indicating extensive dehydration of the coating). At  $200^\circ\text{C}$  the weight of magnesium phosphate is decreased by about 25 %. The reduction in the weight of the sample zinc phosphate crystals is significantly slower.

Based on the data obtained, the conclusions set out in earlier works dealing with the thermal stability of zinc phosphate [20-22] can be confirmed,

i.e. that the dehydration is more gradual and tiered. Conversely, magnesium phosphate dehydrates abruptly, the boundary temperature for rapid dehydration of magnesium phosphate (newberyite) is about 125 °C.

Sharp dehydration of the magnesium phosphate coating after the temperature exceeds approximately 125 °C will result in a significantly greater percentage of cracks and discontinuities in the coating than would be the case of zinc phosphate. After exceeding said temperatures, reduced bond of applied coatings (e.g. thermosetting paint or plasma deposited coatings) can be expected to a greater extent.

Of course, there may be differences in the thermal loading of zinc phosphate [21] as the individual coatings may contain, hopeite (major phase) and significant quantities of phosphophyllite ( $\text{Zn}_2\text{Fe}(\text{PO}_4)_2 \cdot 4\text{H}_2\text{O}$ ). The thermal stabilities of phosphophyllite and hopeite are of cause different.

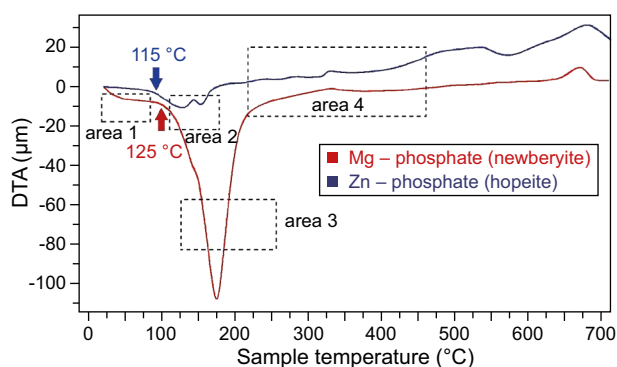


Fig. 5. Comparative record of DTA analysis for magnesium (newberyite) and zinc phosphate (hopeite)  
Obr. 5. Srovnávací záznam DTA termické analýzy pro hořečnatý (newberyite) a zinečnatý fosfát (hopeite)

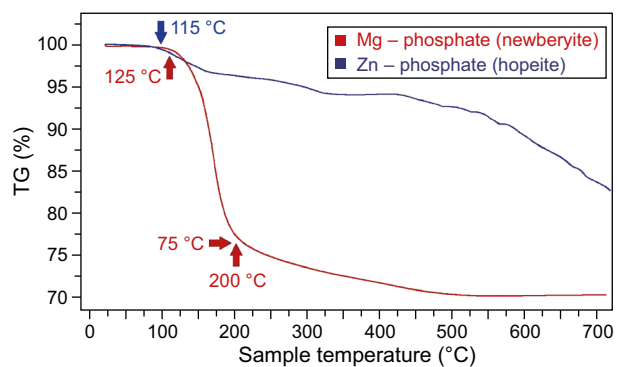


Fig. 6. Comparative record of TG analysis for magnesium (newberyite) and zinc phosphate (hopeite)  
Obr. 6. Srovnávací záznam TG termické analýzy pro hořečnatý (newberyite) a zinečnatý fosfát (hopeite)

## CONCLUSION

Although previous work suggest that coatings of magnesium phosphate (newberyite –  $\text{MgHPO}_4 \cdot 3\text{H}_2\text{O}$ ) on steel substrates provide comparable corrosion resistance as conventional coatings of zinc phosphate (hopeite –  $\text{Zn}_3(\text{PO}_4)_2 \cdot 4\text{H}_2\text{O}$ ), the coatings have very different thermal stability. Magnesium phosphate (newberyite) coatings showed a significant jump in dehydration reaction after reaching a temperature of 125 °C, whereas the dehydration reaction for zinc phosphate remains slow, even after exceeding this temperature. In applications at elevated temperatures, a conventional coating of zinc phosphate (hopeite) is preferred since it has a higher thermal stability against dehydration compared to a magnesium phosphate (newberyite) coating. Alternatively, manganese phosphate coatings (hurealite) can be used for high temperature applications since, according to the technical literature, they have the highest heat (dehydration) resistance.

## Acknowledgement

This research has been supported by Czech Science Foundation project GA ČR No 15-10591S.

## REFERENCES

- Pokorný P, Mastný L, Sýkora V, Pala Z, Brožek V. Bond strength of plasma sprayed ceramic coatings on the phosphated steels, *Metalurgija* **2015**; 54(2), 411–414.
- Narayanan S. Surface pretreatment by phosphate conversion coatings – A review, *Advanced Materials Science* **2005**, 9, 130–177.
- Zimmermann D, Muñoz AG, Schultze JW. Microscopic local elements in the phosphating process, *Electrochimica Acta* **2003**, 48, 3267–3277.
- Banczek EP, Rodrigues PRP, Coasta I. Investigation on the effect of benzotriazole on the phosphating of carbon steel, *Surface and Coating Technology* **2006**, 201, 3701–3708.
- Fang F, Jing J, Tan S, Ma A, Jiang J. Characteristics of a fast low-temperature zinc phosphating coating accelerated by an ECO-friendly hydroxylamine sulfate, *Surface and Coating Technology* **2010**, 204, 2381–2385.
- Kumar A, Bhole SK, Majumdar JD. Microstructural characterization and surface properties of zinc phosphated medium carbon low alloy steel, *Surface and Coating Technology* **2012**, 206, 3693–3699.
- Galvan-Reyes C, Salinas-Rodríguez A, Fuentes-Aceituno JC. Degradation and crystalline reorganization of hurealite crystals during the manganese phosphating of a high strength steel, *Surface and Coating Technology* **2015**, 275, e10–e20.
- Lin B, Lu J. Self-healing mechanism of composite coatings obtained by phosphating and silicate sol post-sealing, *Transactions of Nonferrous Metals Society of China* **2014**, 24, 2723–2728.

9. Pokorný P, Szelag P, Novák M, Mastný L, Brožek V. Thermal stability of phosphate coatings on steel, *Metallurgija* **2015**, 54(3), 489–492.
10. Morks MF. Magnesium phosphate treatment for steel, *Materials Letters* **2004**, 58, 3316–3319.
11. Fouladi M, Amadeh A. Comparative study between novel magnesium phosphate and traditional zinc phosphate coatings, *Materials Letters* **2013**, 98, 1–4.
12. Fouladi M, Amadeh A. Effect of phosphating time and temperature on microstructure and corrosion behavior of magnesium phosphate coatings, *Electrochimica Acta* **2013**, 106, 1–12.
13. Ishizaki T, Shigematsu I, Saito N. Anticorrosive magnesium phosphate coating on AZ31 magnesium alloy, *Surface and Coating Technology* **2009**, 203, 2288–2291.
14. Liu B, Zhang X, Xiao G, Lu Y. Phosphate chemical conversion coatings on metallic substrates for biomedical application: A review, *Materials Science and Engineering C* **2015**, 47, 97–104.
15. Tamini F, Nihouannen D, Bassett D, Ibasco S, Gbureck U, Knowles J, Wright A, Flynn A, Komarova S, Barralet J. Biocompatibility of magnesium phosphate minerals and their stability under physiological conditions, *Acta Biomaterialia* **2011**, 7, 2678–2685.
16. Hivart P, Hauw B. Annealing improvement of tribological properties of manganese phosphate coatings, *Wear* **1998**, 219, 195–204.
17. Hivart P, Hauw B. Seizure behavior of manganese phosphate coatings according to the process conditions, *Tribology International* **1997**, 30(8), 561–570.
18. Wang Ch, Liao H, Tsai W. Effect of heat treatment on the microstructure and electrochemical behavior of manganese phosphate coating, *Materials Chemistry and Physics* **2007**, 102, 207–213.
19. Wang Ch, Liao H, Tsai W. Effect of temperature and applied potential on the microstructure and electrochemical behaviour of manganese phosphate coating, *Surface and Coating Technology* **2006**, 201, 2994–3001.
20. Parthi P, Manivannan V, Kohli S, McCurdy O. Room temperature metathetic synthesis and characterization of  $\alpha$ -hopeite  $Zn_3(PO_4)_2 \cdot 4H_2O$ , *Materials Research Bulletin* **2007**, 43(7), 1836–1841.
21. Pawling O, Trettin R. Synthesis and characterization of  $\alpha$ -hopeite  $Zn_3(PO_4)_2 \cdot 4H_2O$ , *Materials Research Bulletin* **1999**, 34(12/13), 1959–1966.
22. Nomura K, Ujihira Y. Mössbauer spectrometric analysis of thermal decomposition products of phosphate and oxalate coatings on steel, *Journal of Analytical and Applied Pyrolysis* **1983**, 5, 221–236.